

Control of Mobile Manipulator Using Resolved Acceleration with Iterative-Learning-Proportional-Integral Active Force Control

Endra musa

E. Pitowarno¹, M. Mailah²

Abstract – A practical and novel method to control a mobile manipulator is proposed using a resolved acceleration with iterative-learning-proportional-integral active force control strategy. It is implemented as an approach for the robust motion control of a mobile manipulator comprising a differentially driven wheeled mobile platform with a two-link planar arm mounted on top of the platform. The resolved acceleration control is used to manipulate the kinematics of the system in the outermost control loop configuration while the active force control located within the loop is employed to compensate for the dynamic effects including disturbances and uncertainties. The effectiveness and robustness of the proposed scheme is investigated considering a number of introduced disturbances in the forms of impact and vibration forces while the mobile manipulator is performing a trajectory tracking task. The scheme is also validated through an experimental study using a fully developed mobile manipulator prototype. Both theoretical and experimental results verify the viability of the proposed scheme in producing the desired robust motion control performances. Copyright © 2007 Praise Worthy Prize S.r.l. - All rights reserved.

Keywords: Mobile Manipulator, Robust, Resolved Acceleration, Iterative Learning, Active Force Control

I. Introduction

Research on navigating and precise tracking of mobile manipulator (MM) for ultimate motion control involving both the kinematic and dynamic constraints is very challenging and more often than not, an uphill task. The kinematic analysis is particularly useful to describe the robot's workspace and motion path planning tasks including obstacles avoidance, collision free moving capability and maneuverability, while the analysis on the dynamics is specifically targeting the ability of the system to deal with the interaction of masses and forces between the system and its environment as the system moves. Robustness of the system performance seems to be the popular trend in control that demands the dynamic system to perform its task excellently even in the presence of adverse operating and loading conditions.

Solving the kinematics and dynamics' uncertainties in one solution of motion control was known to be very effective and efficient method particularly in real world applications that need precise and robust tracking specifications. There are a number of extensive works that can be found in literature related to the kinematics of the MM, such as those employing homogenous matrices and dual quaternion [1], manipulability extension in local kinematic analysis [2], using the compliant arms analysis for kinematic-based control of multiple mobile manipulators [3] and potential field technique using diffeomorphic transformations and the

resulting point-world topology [4]. Their works are found to be very useful for future developments in coordinated kinematic control, but unfortunately they did not specifically address the robustness issue of the robotic system. Combining both the extensive kinematic and dynamic aspects for an ideal motion control of any dynamical system still remains a complex and challenging problem. In recent years, a number of researchers have contributed to solving this problem using a number of methods such as combining homogenous system theory and adaptive control [5], sub-optimal trajectory planning for the derived robot's dynamics using an iterative algorithm based on gradient functions synthesized in the hierarchical manner [6] and dynamic control using a class of neural network control that is subjected to kinematic constraints.

The iterative learning (IL) algorithm that was attributed to Arimoto [7] was known to be very effective in achieving convergence for the feedback control problems. It is particularly applicable to robotic system due to the fact that most industrial robots by far operate repetitively and their performance is expected to improve gradually with time through the application of the IL technique. Liang and Looze [8] investigated the performance and robustness of the IL algorithm by proposing a non-causal learning controller which guaranteed both robustness and performance for perturbed process. Moon, *et al.* [9] proposed a class of IL algorithm that is combined with a proportional-plus-derivative (PD) controller for a high-g geared industrial

manipulator that performs repeated tasks. A combination of model-based and iterative learning control (ILC) was proposed in [10] as a method to achieve high-quality motion control of direct-drive robots in repetitive motion tasks.

A practical robust controller known as active force control (AFC) has been implemented by Hewit and Burdess [11] that is based on the principle of invariance and classic Newtonian mechanics. This type of controller has been demonstrated to produce very robust and accurate performance with very little computational burden and that it is readily implemented in real-time. This is in stark contrast with other robust control methods which often involve complex algorithms and mathematical models; more often than not, they are restricted to only simulation works in laboratories. Mailah [12] has improvised the AFC strategy to include intelligent mechanisms that are designed to meet the system's performance criteria. Other AFC-based methods have equally showed comparable performance when applied to various dynamical systems [13]-[15]. It is thus the main aim of the study to propose a controller that takes into account the important elements described earlier and applied them to a differentially driven wheeled mobile manipulator.

In this study, a robust motion control scheme applied to the MM system was presented. It comprises a class of kinematic-based controller known as resolved acceleration control (RAC) and an iterative learning proportional-integral active force control (ILPIAFC) that particularly facilitates the dynamics and disturbances. A class of iterative learning technique employing a PI-like function located in the inner part of the AFC loop is designed to cause convergence of the learning process. It was applied using suitable choice of learning constants that in turn lead to the appropriate estimation of the inertial parameters that is vital for the effective compensation of the disturbances. The overall proposed control scheme is to be known as RAC-ILPIAFC and based on this scheme, a simulation and experimental study on the robot model considering both the kinematic and dynamic effects was rigorously performed. Results from both studies show good conformity in that the MM was able to robustly and effectively track the desired trajectories when it is subjected to the introduced impact and vibratory disturbances.

II. Modelling of a Mobile Manipulator

The mobile manipulator considered in this study is illustrated in Fig. 1. It consists of a wheeled mobile platform and a two-link manipulator mounted on top of the platform.

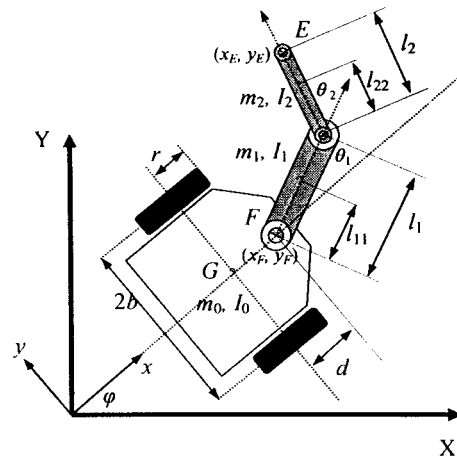


Fig. 1. A mobile manipulator

The platform moves by driving the two independent right and left wheels. The manipulator is constructed as a serial two-link planar arm with servomotors attached at the joints. XY and xy are the world and robot coordinate systems respectively, ϕ is the robot's heading angle, b is the half width of the robot, r is the radius of the wheel, and d is the distance between point G and F . The mass and inertia of the platform are denoted as m_0 and I_0 respectively. For the manipulator, l_1 is the length of link-1, l_{11} is the distance between F to the center of the mass of link-1, l_2 is the length of link-2, l_{22} is the distance between joint-2 to the centre of the mass of link-2. m_1 , m_2 and I_1 , I_2 represent the masses and inertias of link-1 and link-2 respectively. The coordinate of the tip position is denoted by (x_E, y_E) . It is assumed that the velocity at which this system moves is relatively slow and thus the two driven wheels do not slip sideways. The velocity of the platform at the centre of mass, v_G , is then perpendicular to the wheel axis. This expresses x and y components in a nonholonomic manner described by the following equation:

$$\dot{x}_G \sin \phi - \dot{y}_G \cos \phi = 0 \quad (1)$$

For point F , the constraint can be written as:

$$\dot{x}_F \sin \phi - \dot{y}_F \cos \phi + \dot{\phi} d = 0 \quad (2)$$

The kinematic equation of the platform in the form of a rotation matrix can be expressed as:

$$\begin{pmatrix} \dot{x}_F \\ \dot{y}_F \end{pmatrix} = \begin{pmatrix} \cos \phi & -\sin \phi \\ \sin \phi & \cos \phi \end{pmatrix} \begin{pmatrix} \frac{r}{2} & \frac{r}{2} \\ -\frac{d \cdot r}{2b} & \frac{d \cdot r}{2b} \end{pmatrix} \begin{pmatrix} \dot{\theta}_L \\ \dot{\theta}_R \end{pmatrix} \quad (3)$$

Using Eq. (3) for the manipulator mounted on board the platform at point F , its forward kinematic can be described as:

$$\begin{pmatrix} \dot{x}_E \\ \dot{y}_E \end{pmatrix} = \begin{pmatrix} \dot{x}_F \\ \dot{y}_F \end{pmatrix} + \begin{pmatrix} \cos\phi & -\sin\phi \\ \sin\phi & \cos\phi \end{pmatrix} \begin{pmatrix} J_{11} & J_{12} \\ J_{21} & J_{22} \end{pmatrix} \begin{pmatrix} \dot{\theta}_1 + \dot{\phi} \\ \dot{\theta}_2 \end{pmatrix} \quad (4)$$

where:

$$J_{11} = -l_1 \sin\theta_1 - l_2 \sin(\theta_1 + \theta_2) \quad (5)$$

$$J_{12} = -l_2 \sin(\theta_1 + \theta_2) \quad (6)$$

$$J_{21} = l_1 \cos\theta_1 + l_2 \cos(\theta_1 + \theta_2) \quad (7)$$

$$J_{22} = l_2 \cos(\theta_1 + \theta_2) \quad (8)$$

Eq. (4) indicates that the kinematic control of the two sub-systems (platform and manipulator) can be partially solved. It is sometimes very useful to analyze the redundancy of the system when the robot arm is out of reach beyond its workspace. If (x_F, y_F) is assumed to be in a fixed position (platform is not moving and hence $\dot{\phi} = 0$), Eq. (4) can be expressed as:

$$\begin{pmatrix} \dot{x}_T \\ \dot{y}_T \end{pmatrix} = \begin{pmatrix} J_{11} & J_{12} \\ J_{21} & J_{22} \end{pmatrix} \begin{pmatrix} \dot{\theta}_1 \\ \dot{\theta}_2 \end{pmatrix} \quad (9)$$

where (x_T, y_T) is the tip position coordinate relative to the workspace of the manipulator.

Letting $q = [x_F, y_F, x_E, y_E]^T$ as the input reference coordinate and from Eqs. (4) to (9), the total kinematic equation of the mobile manipulator is:

$$\begin{pmatrix} \dot{x}_E \\ \dot{y}_E \\ \dot{x}_F \\ \dot{y}_F \end{pmatrix} = \begin{bmatrix} \cos\phi & -\sin\phi & 0 & 0 \\ \sin\phi & \cos\phi & 0 & 0 \\ 0 & 0 & \cos\phi & -\sin\phi \\ 0 & 0 & \sin\phi & \cos\phi \end{bmatrix} \begin{bmatrix} \frac{r}{2} - J_{11} \frac{r}{b} & \frac{r}{2} + J_{11} \frac{r}{b} & J_{11} & J_{12} \\ -(d + J_{21}) \frac{r}{b} & (d + J_{21}) \frac{r}{b} & J_{21} & J_{22} \\ \frac{r}{2} & \frac{r}{2} & 0 & 0 \\ -d \frac{r}{b} & d \frac{r}{b} & 0 & 0 \end{bmatrix} \begin{bmatrix} \dot{\theta}_L \\ \dot{\theta}_R \\ \dot{\theta}_1 \\ \dot{\theta}_2 \end{bmatrix} \quad (10)$$

where $\dot{\theta}_L$ and $\dot{\theta}_R$ are the angular velocities of the left and right wheels respectively, $\dot{\theta}_1$ and $\dot{\theta}_2$ are the angular velocities of the joints at link-1 and link-2 respectively. A mobile manipulator dynamic equation

can be obtained using the Lagrangian approach [16], [17] in the following form:

$$M(q)\ddot{q} + C(q, \dot{q})\dot{q} + F(q, \dot{q}) + A^T(q)\lambda + \tau_d = B(q)\tau \quad (11)$$

where:

- $q \in \mathfrak{R}^p$ = Generalized coordinate
- $M(q) \in \mathfrak{R}^{p \times p}$ = A symmetric and positive definite inertia matrix
- $C(q, \dot{q}) \in \mathfrak{R}^{p \times p}$ = Centripetal and Coriolis's matrix
- $F(q, \dot{q}) \in \mathfrak{R}^p$ = Friction and gravitational vectors
- $A(q) \in \mathfrak{R}^{r \times p}$ = A constraint matrix
- $\lambda \in \mathfrak{R}^r$ = Lagrange multiplier which denotes the vector of constraint forces
- $\tau_d \in \mathfrak{R}^p$ = Bounded unknown disturbances including unstructured dynamics
- $B(q) \in \mathfrak{R}^{p \times (p-r)}$ = Input transformation matrix
- $\tau \in \mathfrak{R}^{p-r}$ = Torques input vector

For the mobile manipulator considered in this study, the components of friction and gravitational vectors are neglected.

III. Controller Design

The proposed RAC-ILPIAFC controller as shown in Fig. 2 is made up of two main controllers that could be theoretically designed independently. The RAC section is derived based on the previous work done in [18] and is specifically designed to manipulate the kinematics of the mobile manipulator while the ILPIAFC facilitates the dynamic aspects and disturbances to cater for the robustness feature.

III.1. RAC section

The RAC part consists of the five controllers' output equations for $q = [x_F, y_F, \phi, x_E, y_E]^T$ as follows:

$$\ddot{x}_E = \ddot{x}_{ref} + K_d(\dot{x}_{ref} - \dot{x}_{act}) + K_p(x_{Fref} - x_{Fact}) \quad (12)$$

$$\ddot{y}_E = \ddot{y}_{ref} + K_d(\dot{y}_{ref} - \dot{y}_{act}) + K_p(y_{Fref} - y_{Fact}) \quad (13)$$

$$\ddot{\phi}_e = \ddot{\phi}_{ref} + K_d(\dot{\phi}_{ref} - \dot{\phi}_{act}) + K_p(\phi_{ref} - \phi_{act}) \quad (14)$$

$$\ddot{x}_E = \ddot{x}_{ref} + K_d(\dot{x}_{ref} - \dot{x}_{act}) + K_p(x_{Eref} - x_{Eact}) \quad (15)$$

$$\ddot{y}_E = \ddot{y}_{ref} + K_d(\dot{y}_{ref} - \dot{y}_{act}) + K_p(y_{Eref} - y_{Eact}) \quad (16)$$

The subscript *ref*, *act* and *e* refer to the input reference, actual output and error respectively.

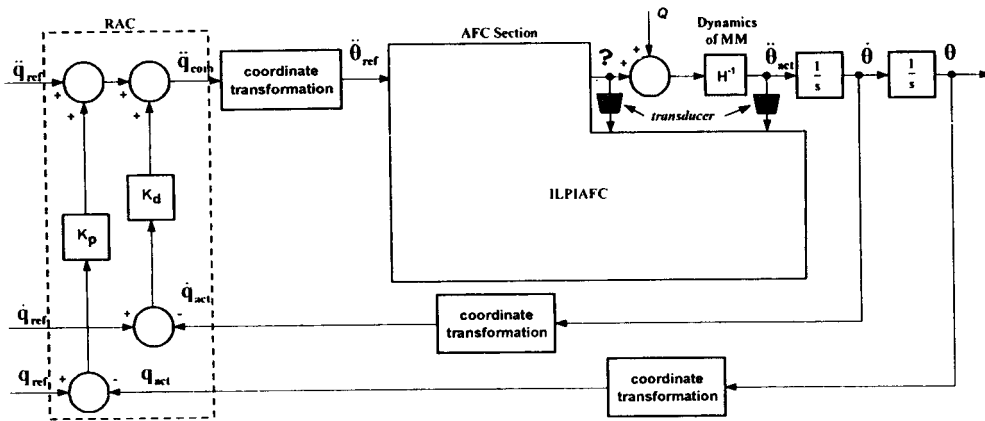


Fig. 2. The proposed RAC-ILPIAFC controller

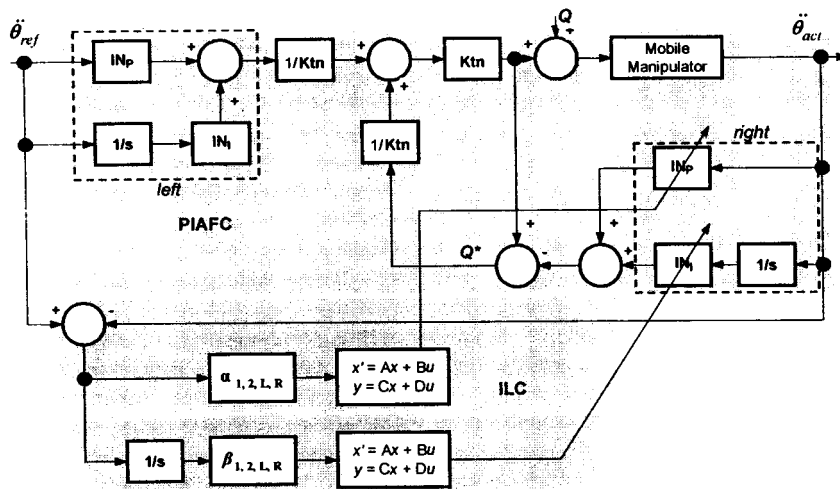


Fig. 3. The proposed ILPIAFC scheme

K_p and K_d are the proportional and derivative gains respectively. For the application of the RAC scheme only, the controller output parameters with subscript e could be directly connected to the actuators input. In the global mobile manipulator motion control, the controller equations can be decoupled and executed simultaneously in real-time. Note that, both forward and inverse kinematic transformation must be carried out to apply the above equations in the control loop. Each output of the above equations is normally passed through a converter prior to the actuation of the system.

III.2. AFC Section

Active force control (AFC) presents a practical and robust method of controlling dynamical systems.

For the MM, AFC was designed to operate in the acceleration mode of the joints and wheels. The AFC method as shown schematically in Fig. 4 relies on the measurement and estimation of selected parameters in order to effect the compensation action of the inner

control (AFC) loop. Physical sensors can be used to acquire the relevant information from the parameters in actual experimentation while in simulation, it is normal to assume perfect modelling of the sensors.

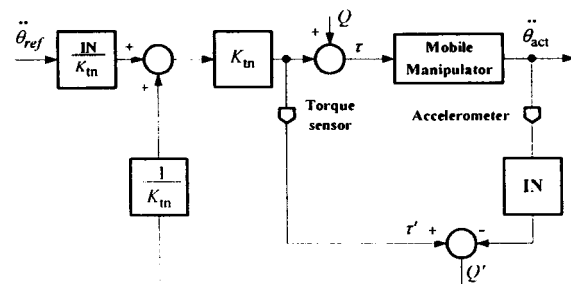


Fig. 4. The AFC scheme

From the Newton's second law of motion for a rotating mass, the sum of all torques (τ) acting on the body is the product of the mass moment of inertia (I)

and the angular acceleration (α) of the body in the direction of the applied torque, can be represented as:

$$\sum \tau = I\alpha \quad (17)$$

For a mobile manipulator system, this can be translated as:

$$\tau + Q = I(\theta)\alpha \quad (18)$$

where τ is the applied torque, Q is the disturbance torque, $I(\theta)$ is mass moment of inertia of the wheels and arms, and θ is the angle at each wheel or joint, α is the angular acceleration. A measurement of Q' as an estimate of Q can be obtained as:

$$Q' = I' \alpha' - \tau' \quad (19)$$

where the superscript ' denotes a measured or computed (or estimated) quantity. The torque τ' can be measured using a physical torque sensor or current sensor (with suitable conversion) while α' using an accelerometer. I' may be acquired through crude approximation method, reference of a look-up table or other suitable techniques [11]. In Fig. 4, I' is denoted as IN . Further developments in methods to estimate the inertia matrix are through the use of artificial intelligence (AI) algorithm such as neural network [12] and knowledge-based system [13]. However, the use of AI in practical applications is usually not that straightforward and more often than not, computationally extensive. Finally, Eq. (19) must pass through a weighting function which is in fact an inverse transfer function of the actuator prior to the summing junction as shown in Fig. 4.

III.3. Proposed ILPIAFC Design

The actuation command for the dynamic control of the mobile manipulator using the PIAFC configuration can be written as [14]:

$$\tau = IN_p (\ddot{\theta}_{ref} - \ddot{\theta}_{act}) + IN_I \int_0^t (\ddot{\theta}_{ref} - \ddot{\theta}_{act}) dt + I'K_m \quad (20)$$

where K_m is the motor torque constant for a torque motor. The above expression can be rewritten in the following form:

$$\tau = \underbrace{IN_p \ddot{\theta}_{ref} + IN_I \int_0^t \ddot{\theta}_{ref} dt}_{left} - \underbrace{IN_p \ddot{\theta}_{act} - IN_I \int_0^t \ddot{\theta}_{act} dt + I'K_m}_{right} \quad (21)$$

The expression in Eq. (21) indicates that the PIAFC output equation contains two groups of the corresponding IN_p and IN_I as can also be observed in Fig. 3. In principle, these IN_p and IN_I were obtained as the optimum values for the general robot operation and working conditions. Referring to Fig. 3 and considering the adaptation is only applied to the right hand side of the PIAFC expression of Eq. (21), it can be rewritten as:

$$\tau = IN_{pF} \ddot{\theta}_{ref} + IN_{IF} \int_0^t \ddot{\theta}_{ref} dt - IN_{pV} \ddot{\theta}_{act} - IN_{IV} \int_0^t \ddot{\theta}_{act} dt + I'K_m \quad (22)$$

where IN_{pF} is the fixed IN_p , IN_{IF} is the fixed IN_I , and IN_{pV} and IN_{IV} are the varied IN_p and IN_I respectively. In this case, the IN_{pV} and IN_{IV} will be supplied by the IL control algorithm. Eq. (22) is considered as the main dynamics for the proposed ILPIAFC scheme with the learning update law as follows:

$$u_j(k) = u_{j-1}(k) + \gamma e_{j-1}(k+1) \quad (23)$$

where γ is a PI-type of IL control and is defined as:

$$\gamma(s) = \alpha + \frac{\beta}{s} \quad (24)$$

where α and β are proportional and integral constants (or the learning parameters) of the ILC algorithm that are configured as:

$$\alpha = [\alpha_{motor-1} \quad \alpha_{motor-2} \quad \alpha_{motor-L} \quad \alpha_{motor-R}]^T \quad (25)$$

and:

$$\beta = [\beta_{motor-1} \quad \beta_{motor-2} \quad \beta_{motor-L} \quad \beta_{motor-R}]^T \quad (26)$$

The output function $u_j(k)$ facilitates the adaptation of the inertia matrix of the respective joints and wheels of the MM system.

In this ILC scheme, the acceleration error, $(\ddot{\theta}_{ref} - \ddot{\theta}_{act})$ is defined as the learning input.

IV. Simulation

Simulation was performed using MATLAB and Simulink software package.

Fig. 5 shows a Simulink model of the proposed control scheme showing the details of the system comprising the input function, controllers, inverse and direct kinematics, dynamics of the mobile manipulator and the controller selector.

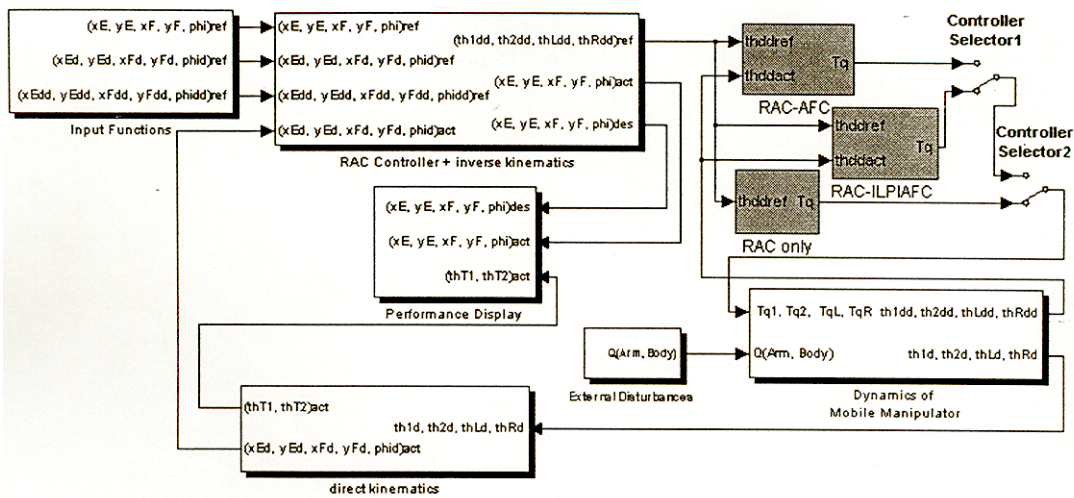


Fig. 5. The Simulink model of the RAC, RAC-AFC and proposed RAC-ILPIAFC

It should be noted that the simulation study was performed considering three schemes, i.e. RAC only, RAC-AFC and RAC-ILPIAFC so that useful comparison can be made. A selector switch has been added to facilitate the three controller modes.

The task of the MM is to drive its platform in a circular motion (trajectory) with a curvature radius of 10 m, at a speed of 0.2 m/s (subjected to point F) and the initial heading angle orientation $\pi/2.4$ relative to the zero angle of the world Cartesian coordinate. The manipulator is defined to follow a pre-defined curve track at the right-hand side of the platform starting from the world Cartesian coordinate (10.41, 0.35). The initial tip position is set to point (10.55, 0.35).

The initial experiment was to determine the appropriate values of K_p and K_d of the RAC section. The tuning process was performed in the RAC mode using heuristic method considering some disturbances in the process. By using the tuned K_p and K_d values, a number of experiments was then performed to include the AFC and ILPIAFC schemes.

The (basic) IN of the RAC-AFC scheme was also approximated in the same manner. For the mobile platform, the range of the IN value from 1 to 2.8 kgm^2 was optimized manually with a step of 0.1 kgm^2 . For the manipulator, it was optimized in the range from 0.0600 to 0.100 kgm^2 with an incremental step of 0.005 kgm^2 .

Finally, by completing the tuning process for RAC and RAC-AFC, the adaptation of IN_p and IN_i in the RAC-ILPIAFC mode can be performed.

V. Results and Discussion

From the initial investigation, the optimum K_p and K_d values of the RAC for $q = [x_F, y_F, \phi, x_E, y_E]^T$ were obtained as follows:

$$K_p = \text{diag}\{450 \ 450 \ 0.004 \ 325 \ 325\}$$

$$K_d = \text{diag}\{320 \ 320 \ 0.001 \ 260 \ 260\}$$

It should be noted that the K_p and K_d values (0.004 and 0.001 respectively) for the robot's heading angle control are relatively very small compared with those of the robot's movement control. This is due to the fact that the heading angle control is very sensitive in the proposed (x, y, ϕ) kinematic control mode. These control parameter values would subsequently be used in the next investigation employing the AFC and ILPIAFC schemes. The tuned IN value was obtained as:

$$\text{IN} = \text{diag}\{0.0925 \ 0.0925 \ 2.4 \ 2.4\}$$

This value was then used as the reference IN value for testing the robustness of the proposed RAC-AFC scheme. The IN_p and IN_i were then tuned by considering only a small value adjustment that based on the tuned IN, and the results obtained are as follows:

$$\text{IN}_p = \text{diag}\{0.125 \ 0.125 \ 2.4 \ 2.4\}$$

$$\text{IN}_i = \text{diag}\{0.03 \ 0.03 \ 0.01 \ 0.01\}$$

At this point, the iterative-learning algorithm can be activated by implementing the tuned IN_p and IN_i as the initial conditions of the learning process. First, the elements of the Markov system parameters (see the blocks of the state-space equations in Fig. 3) - A , B and C in matrix P were respectively chosen as 0.05, 0.2, and 0 respectively. It should be noted that D was also set to 0. Actually, A , B and C can be set to any value that satisfy $|1 - \gamma CB| < 1$ as described by Arimoto [7]. Next, α and β were tuned and the results are given as:

$$\alpha = \text{diag}\{0.45 \ 0.45 \ 0.06 \ 0.06\}$$

$$\beta = \text{diag}\{0.03 \ 0.03 \ 0.005 \ 0.005\}$$

In experimenting the system robustness, there are two types of disturbances considered in the study. The first is the impact force and another vibratory excitation that are correspondingly applied to each wheel (platform) and joint (arm) of the mobile manipulator. Figs. 6(a) to (c) show illustrations of the introduced disturbances.

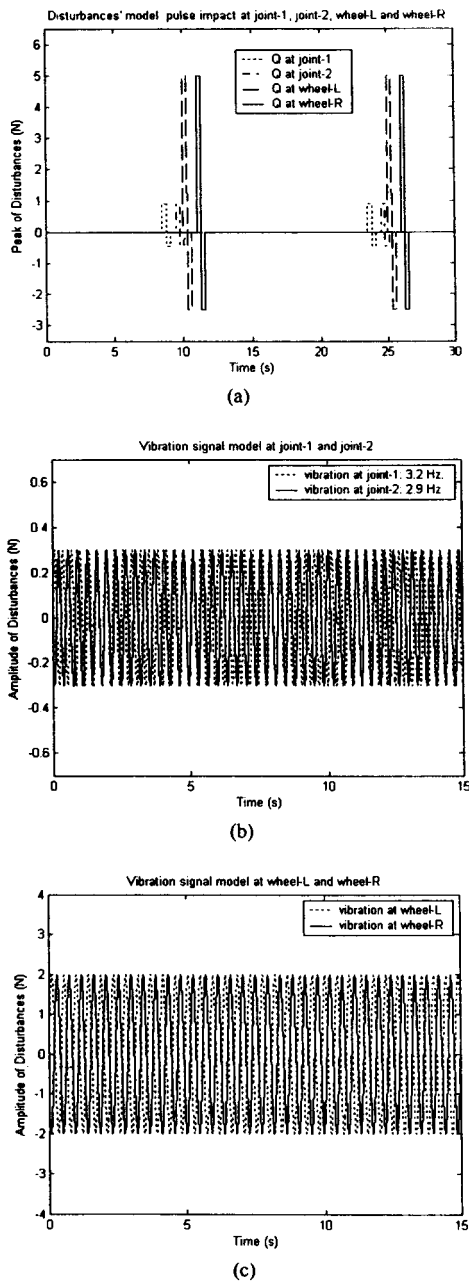


Fig. 6. Introduced disturbances on the mobile manipulator: (a) impact disturbances, (b) vibration at the arm and (c) vibration at the wheels

The impact forces were introduced to joint-1, joint-2, wheel-L and wheel-R as shown in Fig. 6(a).

It emulates the condition of the MM at an instant when the wheels are encountering abrupt changes in the surface terrain such as bumps or holes. Vibration excitation is also applied to each wheel considering amplitude of $\pm 2\text{N}$ and at frequency of 2.2 Hz. This condition is synonymous to MM navigating on a very wavy surface terrain. In addition, further vibration disturbances at joint-1 and joint-2 of the arm with the following specifications: 3.2 Hz, $\pm 0.3\text{N}$ and 2.9 Hz, $\pm 0.3\text{N}$ respectively were introduced.

Figs. 7(a) and (b) show the performance of the RAC and RAC-AFC schemes respectively due to the vibration effects. The track errors generated through the AFC based scheme is far less than the RAC counterpart.

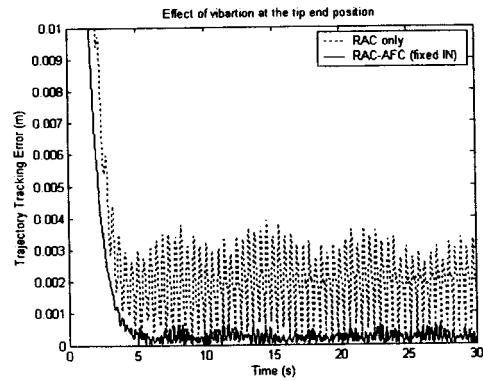


Fig. 7(a). Effect of vibration at the tip of the arm

The average track error of the arm for the RAC method is around 3 mm whereas for the RAC-AFC, the error is successfully suppressed to less than 1 mm mark. The superiority of the AFC-based scheme is thus obvious and verified.

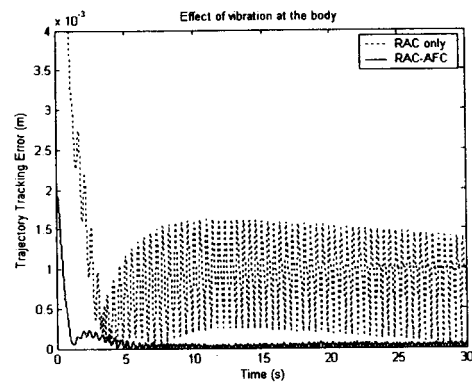


Fig. 7(b). Effect of vibration at the body

Figs. 8(a) and (b) illustrate the effects of vibration for the RAC-AFC and RAC-ILPIAFC schemes.

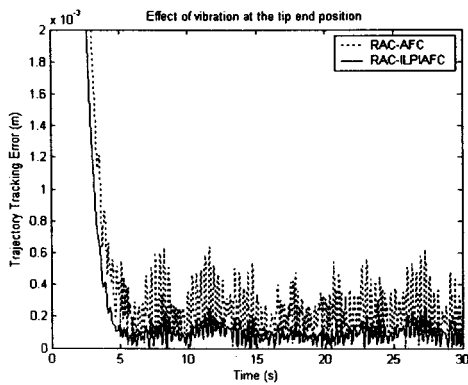


Fig. 8(a). Effect of vibration at the tip of the arm

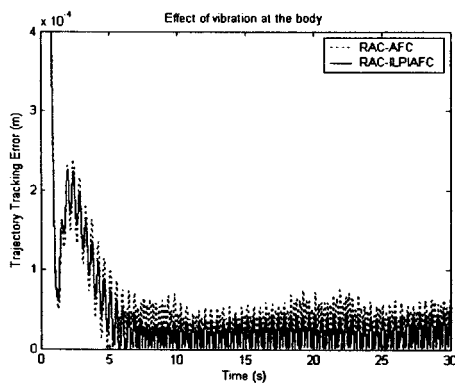


Fig. 8(b). Effect of vibration at the body (point *F*)

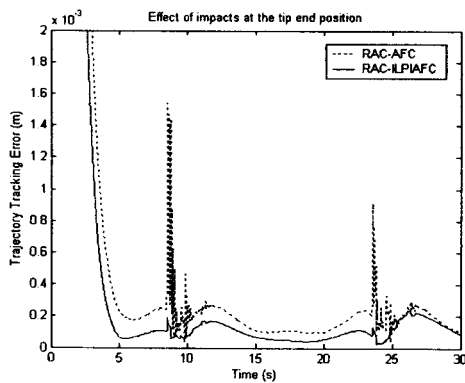


Fig. 9(a). Effect of impacts at the tip position

From Fig. 8(a), it is clear that the incorporation of adding in the integral term and combined with an iterative learning technique into the AFC has significantly improved the overall performance. The vibration effects that occurred at peaks of around 0.6 mm for the RAC-AFC scheme has been rejected to the level of less than 0.2 mm (average). The IL algorithm plus the PI term is thus shown to be very effective in bringing down the track error. Another test on the system robustness of the RAC-ILPIAFC scheme

through the effect of impact disturbances can be observed in Figs. 9(a) and (b). Fig. 9(a) depicts the effects of the impacts on the tip of the manipulator in which the disturbance was significantly rejected by the proposed RAC-ILPIAFC (indicated by the solid line). The effect of the impacts on the body at point *F* can also be seen in Fig. 9(b). Again, the proposed scheme performs better but this time the difference is not that significant.

Fig. 10 shows the animation of MM when it is executing the given task

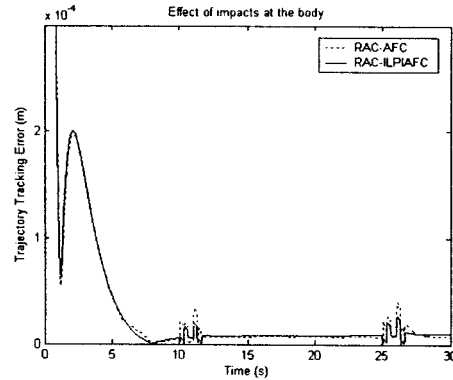


Fig. 9(b). Effect of impacts at the body (point *F*)

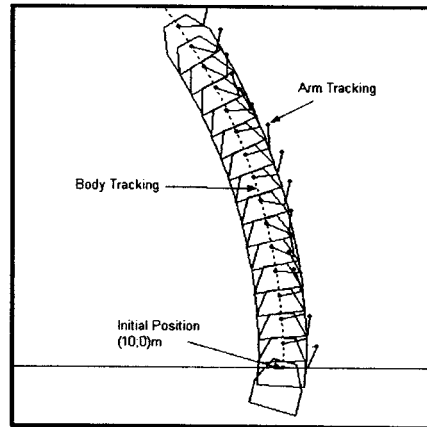


Fig. 10. MM tracking animation

VI. Experimental Study

The effectiveness of the proposed RAC-ILPIAFC was also tested and validated using the fully developed mobile manipulator prototype as shown in Fig. 11. The physical MM was designed and developed by taking into account the parameters already defined in the simulation.

A number of physical constraints on the hardware were also considered.

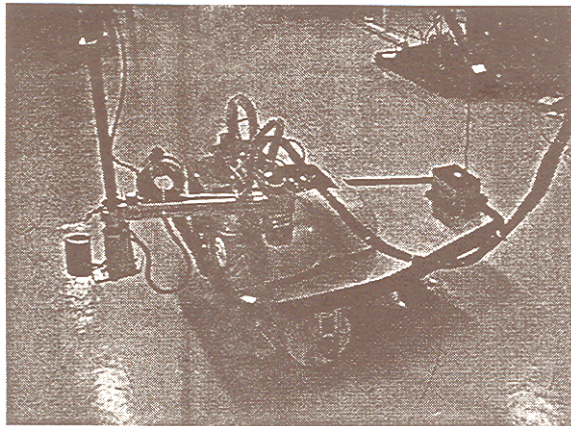


Fig. 11. A photograph of the mobile manipulator prototype

Fig. 12 shows a schematic diagram of the PC-based mobile manipulator control employed in the prototype. Two data acquisition cards (both using DAS-1602 model) based on a P-III IBM PC were used to manipulate 12 channels of analogue inputs and four channels of analogue outputs. In addition, the rig was also designed to operate using the microcontroller system by dismantling the PC-based controller (indicated by the dash box) and replacing it with the PIC16F877 embedded controller.

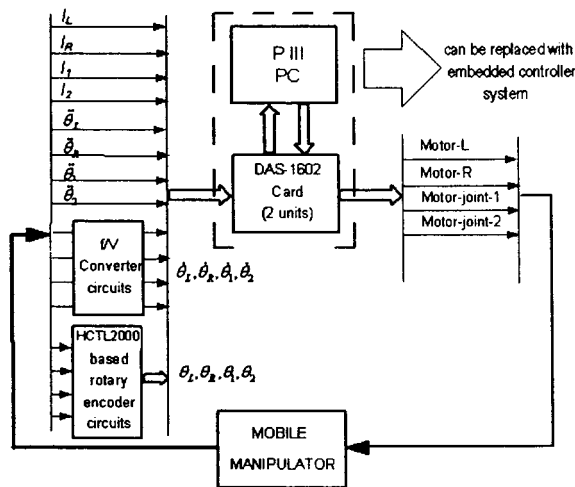


Fig. 12. The schematic diagram of the PC-based MM control

Some of the programs written in C that were derived from the theoretical section and later included in the simulation were subsequently used in the experiments both for the PC-based and microcontroller-based systems. On top of that, a number of experiments were also developed using the Real-Time Workshop (RTW) facility in conjunction with the Simulink program. In this case, the DAS-1602 card should be properly configured according to the Simulink block diagrams and functions to take into account the actual inputs (sensors) and outputs (motors). Fig. 13 shows a display

window of the Real Time Control and Monitor of MM's AFC Online System (RTCM-MMAFC-OS) that was developed in the study. Through this interactive display, users can set the control parameter values appropriately. When the robot is operating, the tracking process plus its error curves, and the system's sensors measurement can be monitored on the screen in real-time. The graph located in the middle of the window shows the online trajectory tracking of the MM. The inner circle constitutes the body (platform) tracking, while the outer curve (like petals of flower) shows the arm tracking at the tip position. The graph at the top right hand corner of the window shows the online track errors generated by the system.

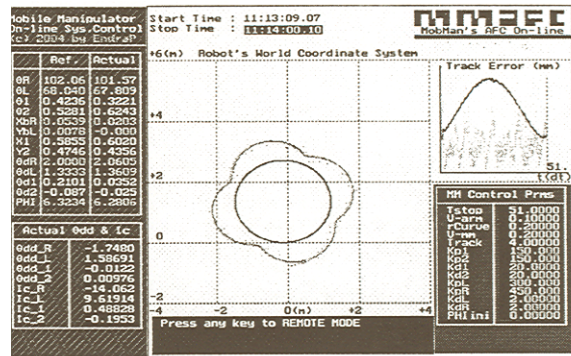


Fig. 13. A display of the RTCM-MMAFC-OS

Generally, for the given robot overall dimension of 80 × 80 cm and the task of tracking a curve with a 10 m radius (or 1.5 m in the experiments), the track errors generated for the control schemes are not at all significant considering a perfectly normal mobile manipulator movement. In simulation, it has been shown that the average track errors are less than 3 mm for all schemes including the RAC only scheme. However, for a high precision robot task, the contribution of the RAC-ILPIAFC method is obvious as it further refines the errors and hence it has real world implication as far as robustness-cum-accuracy application is concerned.

VII. Conclusion

The effectiveness and robustness of the proposed RAC-ILPIAFC has been demonstrated in this study. Combining the RAC with ILPIAFC to the motion control of mobile manipulator is thus considered a new and novel approach in this area of study. The potentials of the RAC-ILPIAFC method particularly as a disturbance rejection scheme were clearly demonstrated in the study, both through simulation as well as practical implementation. The capability of the iterative learning process was particularly highlighted in the study that clearly implies the convergence of the system track errors as learning takes place. The experimental study

shows the feasibility of the proposed control algorithm to be implemented in real-time. However, further experimentation needs to be carried out to explore the maximum potentials of the scheme when other different tasks, parameters or operating and loading conditions are considered.

Acknowledgements

We would like to thank the *Malaysian Ministry of Science and Technology and the Environment (MOSTE)*, *Universiti Teknologi Malaysia (UTM)* and *Institut Teknologi Sepuluh Nopember (ITS)*, Surabaya - Indonesia, for their continuous support in the research work. This research was fully supported by an IRPA grant (No. 03-02-06-0038EA067).

References

- [1] C. Perrier, P. Dauchez, F. Pierrot, *A Global Approach for Motion Generation of Nonholonomic Mobile Manipulator*, Proc. IEEE Int'l Conf. On Robotic & Automation, 1998, pp. 2971-2976.
- [2] B. Bayle, J.Y. Fourquet, M. Renaud, *Manipulability Analysis for Mobile Manipulators*, Proc. IEEE Int'l Conf. On Robotics & Automation, 2001, pp. 1251-1256.
- [3] T.G. Sugar, V. Kumar, *Control of Cooperating Mobile Manipulators*. *IEEE Trans. Robotic and Automation*, Vol. 18, n. 1, pp. 94-103, 2002.
- [4] H.G. Tanner, *Nonholonomic Navigation and Control of Cooperating Mobile Manipulators*, *IEEE Trans. Robotic and Automation*, Vol. 19, n. 1, pp. 53-61, 2003.
- [5] R. Colbaugh, *Adaptive Stabilization of Mobile Manipulator*, Proc. American Control Conf., 1998, pp. 1-5.
- [6] A. Mohri, S. Furuno, M. Iwamura, M. Yamamoto, *Sub-optimal Trajectory Planning of Mobile Manipulator*, Proc. IEEE Int'l Conf. On Robotics & Automation, 2001, pp. 1271-1276.
- [7] S. Arimoto, *Bettering Operation of Dynamic Systems by Learning: A New Control Theory for Servomechanism and Mechatronics Systems*, Proc. 23rd IEEE CDC, Las Vegas, 1984, pp.
- [8] Y.J. Liang, D.P. Looze, *Performances and Robustness Issues in Iterative Learning Control*, Proc. 32nd Conf. Decision and Control, 1993, pp. 1990-1995.
- [9] J.H. Moon, T.Y. Doh, M.J. Chung, *An Iterative Learning Control Scheme for Manipulators*, Proc. IEEE IROS, 1997, pp. 759-765.
- [10] B. Bukkems, D. Kostic, B. Jager, M. Steinbuch, M., *Learning-Based Identification and Iterative Learning Control of Direct-Drive Robots*, *IEEE Trans. Control Systems Technology*, Vol. 13, n. 4, pp. 537-549, 2005.
- [11] J.R. Hewit, J.S. Burdess, *Fast Dynamic Decoupled Control for Robotics using Active Force Control*. *Trans. Mechanism and Machine Theory*, Vol. 16, n. 5, pp. 535-542, 1981.
- [12] M. Mailah, *Intelligent Active Force Control of a Rigid Robot Arm Using Neural Network and Iterative Learning Algorithms*, Ph.D Thesis, University of Dundee, UK, 1998.
- [13] E. Pitowarno, M. Mailah, H. Jamaluddin H, *Knowledge-based Trajectory Error Pattern Method Applied to an Active Force Control Scheme*, *IJUM Engineering Journal*, Vol. 3, n. 1, pp. 1-15, 2002.
- [14] M. Mailah, E. Pitowarno, H. Jamaluddin, *Robust Motion Control for Mobile Manipulator Using Resolved Acceleration and Proportional-Integral Active Force Control*. *International Journal of Advanced Robotic Systems*, Vol. 2, n. 2, pp. 125-134, 2005.
- [15] M. Mailah, G. Priyandoko, *Simulation of A Suspension System With Adaptive Fuzzy Active Force Control*, *International Journal on Simulation Modelling*, Vol. 6, n.1, pp. 25-36, 2007.
- [16] Y. Yamamoto, X. Yun, *Effect of the Dynamics Interaction on Coordinated Control of Mobile Manipulators*, *IEEE Trans. On Robotic and Automation*, Vol. 12, n. 5, pp. 816-824, 1996.
- [17] S. Lin, A.A. Goldenberg, *Neural Network Control of Mobile Manipulators*, *Trans. Neural Networks*, Vol. 12, n. 5, pp. 1121-1133, 2001.
- [18] J. Y. S. Luh, M. W. Walker, R.P.C. Paul, *Resolved Acceleration Control of Mechanical Manipulator*, *IEEE Trans. Automatic Control*, Vol. 25, pp. 486-474, 1980.

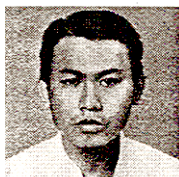
Authors' information

¹Electronics Engineering Polytechnic Institute of Surabaya (EEPIS), Institut Teknologi Sepuluh Nopember (ITS), 60111 Sukolilo – Surabaya, INDONESIA, Tel: +6231-594-7280; Fax: +6231-594-6114 E-mail: epit@eepis-its.edu

²Department of Applied Mechanics, Faculty of Mechanical Engineering, Universiti Teknologi Malaysia (UTM), 81310 Skudai – Johor, MALAYSIA, Tel: +607-553-4562; Fax: +607-556-6159 E-mail: musa@fkm.utm.my



Endra Pitowarno was born in Bondowoso, Surabaya, Indonesia on the 30th of June 1962. He obtained his Bachelor Degree in Electrical and Electronics Engineering from the Institut Teknologi Sepuluh Nopember, Surabaya, Indonesia in 1986 before acquiring Masters of Engineering and Philosophy of Doctorate qualifications from the Universiti Teknologi Malaysia in 1999 and 2005 respectively both in Mechanical Engineering. His major field of study is robotic and mechatronics.



Musa Mailah was born in Singapore on the 28th of June 1963. He obtained his Bachelor Degree in Mechanical Engineering from the Universiti Teknologi Malaysia, Malaysia, in 1988 before acquiring Masters of Science and Philosophy of Doctorate qualifications from the University of Dundee, UK in 1992 and 1998 respectively both in Mechatronics. His major field of study is robot control and mechatronics.

He is currently a senior lecturer at the Institut Teknologi Sepuluh Nopember, Surabaya, Indonesia and his research interests include applied mechatronics and embedded systems.

He is currently an Associate Professor at the Universiti Teknologi Malaysia and his research interests include intelligent active force control of dynamical systems, applied mechatronics, system modelling and simulation.